Nanoscale

Cite this: *Nanoscale*, 2012, **4**, 3438

www.rsc.org/nanoscale

PAPER

A highly sensitive electrochemical biosensor based on zinc oxide nanotetrapods for L-lactic acid detection

Yang Lei,[ab] Ning Luo,[a] Xiaoqin Yan,*[a] Yanguang Zhao,[a] Gong Zhang[a] and Yue Zhang*[ac]

Received 12th February 2012, Accepted 20th March 2012
DOI: 10.1039/c2nr30334e

An amperometric biosensor based on zinc oxide (ZnO) nanotetrapods was designed to detect L-lactic acid. The lactate oxidase was immobilized on the surface of ZnO nanotetrapods by electrostatic adsorption. Unlike traditional detectors, the special four-leg individual ZnO nanostructure, as an adsorption layer, provides multiterminal charge transfer channels. Furthermore, a large amount of ZnO tetrapods are randomly stacked to form a three-dimensional network naturally that facilitates the exchange of electrons and ions in the phosphate buffer solution. Utilizing amperometric response measurements, the prepared ZnO nanotetrapod L-lactic acid biosensor displayed a detection limit of 1.2 μM, a low apparent Michaelis–Menten constant of 0.58 mM, a high sensitivity of 28.0 μA cm^{-2} mM^{-1} and a good linear relationship in the range of 3.6 μM–0.6 mM for the L-lactic acid detection. This study shows that the biosensor based on ZnO tetrapod nanostructures is highly sensitive and able to respond rapidly in detecting lactic acid.

1. Introduction

Lactic acid, a carboxylic acid with a hydroxyl group, exists widely in the metabolins of humans, animals and microorganisms. L-(+)-Lactic acid, one of the two optical isomers of lactic acid, is very important biologically. By detecting the L-lactate level of human blood and tissues, various pathological states, such as shock, suffocation, carbon monoxide or cyanide intoxication, heart or liver diseases, and particularly, the physical conditions of athletes, can be evaluated. Because of the importance of L-lactic acid in disease diagnosis, dairy and alcoholic beverage industries, sport medicines, and degradable raw materials, great attention to designing a simple, rapid and sensitive device for L-lactic acid detection has been aroused.[1,2]

Spectrophotometry is involved in traditional determination of L-lactic acid level of human blood and tissues in the disease diagnosis field.[3] However, this laboratory spectroscopic technique is relatively costly, time-consuming, hard to implement and needs large sample quantities. Therefore, another conventional method for monitoring lactate levels, which makes use of electrochemical enzyme electrode detection, is considered to be more suitable for developing inexpensive portable devices. This method has the advantages of good selectivity, rapid response, simple and direct measurements, reproducible results, as well as miniature size and online monitoring. In this method, there are four different kinds of enzymes suitable for L-lactic acid determination: lactate dehydrogenase (LDH), cytochrome b_2 (Cyt b_2), lactate oxidase (LOD), and lactate monooxygenase (LMO). Recently, LOD has been mostly selected in amperometric biosensor applications,[4–6] because its catalytic process is relatively simple and no coenzyme is needed. Moreover, only oxygen is required in this reaction. Therefore, LOD was chosen to catalyze L-lactic acid in this study.

Regarding LOD enzyme electrode configurations, the biorecognition element LOD needs to be fixed on the electrodes. It is well-known that sensitivity and selectivity of the electrochemical biosensor can be considerably enhanced by modifying the surface of the working electrode with conducting copolymers,[7] ionotropic gelation of biopolymers,[8] mucin/albumin hydrogel matrix,[9] polypyrrole,[10] *etc.* Recently, nanomaterials with novel properties have been considered for immobilizing LOD, such as carbon nanotubes,[10] hydrogen titanate nanotubes,[11] and platinum nanoparticles.[12] Among numerous nanomaterials, zinc oxide (ZnO) with good biocompatibility and high-charge transporting abilities is one of the most applicable materials for binding the enzyme. With a high isoelectric point (IEP 9.5), it can immobilize LOD with low IEP (4.6) firmly through electrostatic interactions. Meanwhile, ZnO nanostructures offer direct charge conduction tunnels between enzymic active sites and the electrode surface without a mediator.[13–15]

ZnO nanostructures, such as nanoparticles,[16] nanowires,[17] nanotube arrays,[18] nanofibers,[19] nanorods,[20] nanotetrapods,[21] *etc.*, have been studied to construct biosensors, which are mostly for glucose detection. The disorderly arranged ZnO

[a]*State Key Laboratory for Advanced Metals and Materials, School of Materials Science & Engineering, University of Science & Technology Beijing, Beijing 100083, PR China. E-mail: yuezhang@ustb.edu.cn; xqyan@mater.ustb.edu.cn; Fax: +86 10 62333113; Tel: +86 10 62334725*
[b]*Department of Energy Materials & Technology, General Research Institute for Non-ferrous Metals, Beijing 100088, PR China*
[c]*Key Laboratory of New Energy Materials and Technologies, University of Science & Technology Beijing, Beijing 100083, PR China*

nanotetrapods, with unique three-dimensional (3D) structures, can naturally form a network structure as an enzyme adsorption layer.[21,22] This special structure benefits diffusion of electrons and ions in the solutions. In this study, a simple multiterminal electron conduction biosensor has been designed with ZnO nanotetrapods and used to detect L-lactic acid. In order to immobilize more LOD on the electrode surface to enhance the detection performance, the support layer for adsorption of the enzyme requires larger surface area and more active sites. ZnO nanotetrapod was used in this device, providing a 3D spatial network structure and six electron conduction ways in theory.

2. Results and discussion

2.1. Characterization of ZnO nanotetrapods

Fig. 1a shows a typical SEM image of the ZnO nanotetrapods sample under low magnification. It is noticed that the ZnO products have a tetrapod-like nanostructure with a single morphology and uniform length of around 5 μm for each leg. The special structure of the nano-product prepared can be distinctly observed in Fig. 1b (high magnification). The product presents a characteristic structure with four legs growing from a central junction. The leg is about 500 nm in diameter at the base and becomes needle-like at the top end.

The structure of the ZnO nanotetrapods was determined by XRD and Raman spectroscopy. Fig. 1c shows the XRD pattern of the products. Compared with the standard XRD data file (JCPDS 36-1451), the XRD pattern matches well. All the diffraction peaks can be indexed to the ZnO hexagonal wurtzite phase with lattice constants $a = 0.325$ nm and $c = 0.520$ nm. No other crystalline forms were observed. According to the Raman spectrum of the ZnO nanotetrapods shown in Fig. 1d, the two highest peaks for E_2^{low} and E_2^{high} modes appear at 98 cm^{-1} and 438 cm^{-1}, respectively. The peak position of E_2^{low} mode has shifted, compared with the reported ZnO bulk materials (101 cm^{-1}),[23] which may result from the distinctive structure and size of ZnO nanotetrapods.[24] The two weaker peaks at 331 cm^{-1} and 378 cm^{-1} are identified with E_2^{high}–E_2^{low} and A_1(TO) modes, respectively. No other crystalline forms were found consistent with the result of the XRD pattern.

2.2. Electrochemical characterization

Generally, for a LOD-based lactate biosensor, lactate acid is catalyzed by LOD and oxidized into pyruvate. The catalytic reaction at the electrode is described as follows:[25]

$$\text{L-lactic acid} + O_2 \rightarrow \text{pyruvate} + H_2O_2$$

$$H_2O_2 \rightarrow O_2 + 2H^+ + 2e^-$$

The species generated in this reaction is H_2O_2, which can be detected at the electrode. This type of oxidation process has been proven to be more effective and sensitive in detecting substrates.[20,21] Nevertheless, extensive oxidation of the lactic acid can be affected by the structures and properties of conductive electrodes. Therefore, the electrocatalytic activities of the Nafion/LOD/ZnO/Au electrode to L-lactate need to be investigated. The effect of ZnO nanotetrapods on the electric conductivity of the enzyme membrane was evaluated by cyclic voltammetry (CV). The performances of the Nafion/Au electrode (black curve) and the Nafion/LOD/Au electrode (red curve) in the phosphate buffer solution (PBS) (pH 7.4) are nearly the same, as shown in Fig. 2a. Compared with them, the Nafion/LOD/ZnO/Au electrode (blue curve) has better current response in the PBS. It has two obvious peaks of oxidation and reduction at approximately

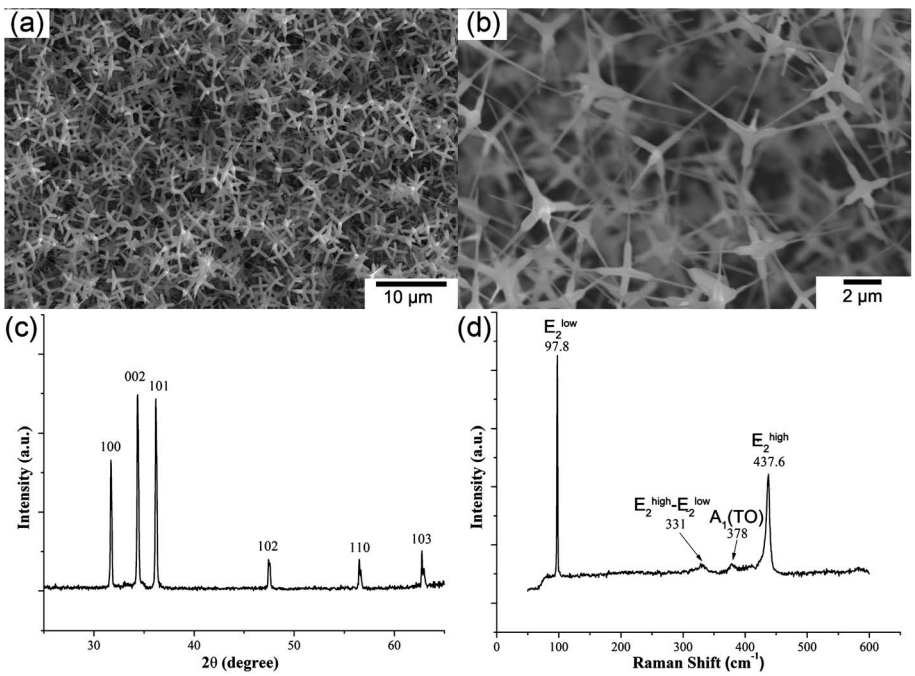

Fig. 1 (a) Low and (b) high magnification SEM images, (c) XRD pattern and (d) Raman spectrum of the prepared ZnO nanotetrapods, respectively.

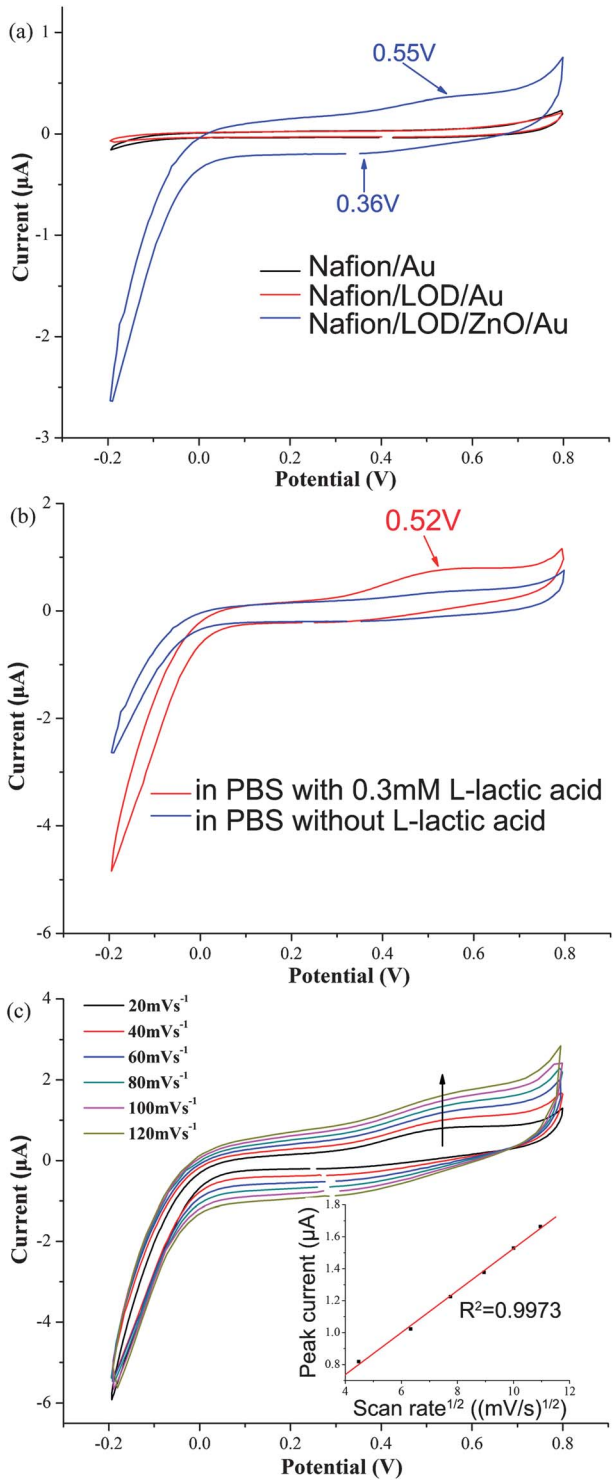

Fig. 2 CV curves of (a) the Nafion/Au electrode (black curve), the Nafion/LOD/Au electrode (red curve) and the Nafion/LOD/ZnO/Au electrode (blue curve) in the PBS at a scan rate of 50 mV s^{-1}, (b) the Nafion/LOD/ZnO/Au electrode in the PBS (blue curve) and in 0.3 mM L-lactic acid (red curve), and (c) the Nafion/LOD/ZnO/Au electrode in the PBS containing 0.3 mM L-lactic acid obtained at various scan rates of 20, 40, 60, 80, 100 and 120 mV s^{-1}, respectively. The inset shows relevant linear relation of peak currents and square roots of scan rates.

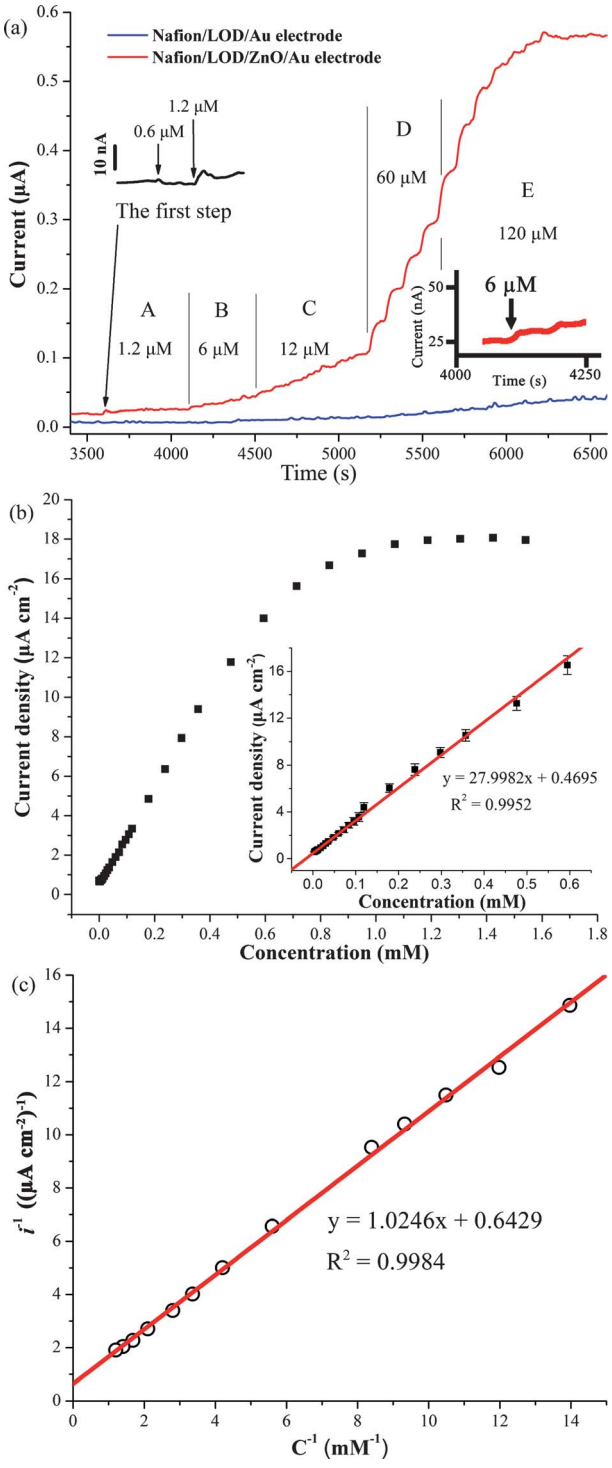

Fig. 3 (a) The response current in real-time for the Nafion/LOD/ZnO/Au electrode (red curve) and the Nafion/LOD/Au electrode (blue curve) in the PBS with addition of L-lactic acid concentrations at 800 mV. The insets show the plots of the response currents in the low concentration regions. (b) The corresponding calibration curve of the response currents *versus* the L-lactic acid concentrations and the inset shows the linear fitting curve. (c) The corresponding Lineweaver–Burk plot. The straight line is the linear fit to the plot.

Table 1 Comparison of performance of various L-lactic acid electrochemical biosensors

Enzyme electrode type	Sensitivity ($\mu A\ cm^{-2}\ mM^{-1}$)	Detection limit (μM)	Linear range (mM)	Response time (s)	Reference
ZnO nanotetrapods	28.0	1.2	0.0036–0.6	10 (90%)	Our work
Nylon net on an oxygen probe	—	—	0.02–0.2	—	4
Pt–Ag/AgCl thin film	0.07	—	0.5–20	<120	5
Ppy–enzyme–CNT nanocomposite-modified Pt	—	10	—	—	10
Hydrogen titanate nanotubes	0.24	200	0.5–14	<5 (90%)	11
Multi-walled CNT/Pt nanoparticle modified GCE	6.36	0.3	0.2–2.0	<5	12
Carbon fiber microelectrodes	9.15 ± 0.91	—	0.1–2.0	—	29
Electrode arrays by hydrogel photolithography	1.1	—	0–10	<70 (90%)	30

0.55 V and 0.36 V in the CV curve, respectively. It is evident from the plot that ZnO nanotetrapods have a significant influence on the semipermeable Nafion-modified enzyme electrode. They provide more conductive paths from the enzyme to the electrode, and therefore improve the electron transfer of the enzyme electrode.

Fig. 2b illustrates the difference of CV curves between the Nafion/LOD/ZnO/Au electrode in the PBS (pH 7.4) with and without 0.3 mM L-lactic acid. The current increases from 0.3 to 0.52 V in the 0.3 mM L-lactic acid solution compared with that in the PBS without L-lactic acid. This is ascribed to the catalytic reaction of the Nafion/LOD/ZnO/Au electrode with L-lactic acid. An evident peak appears at about 0.52 V on the CV curve for the Nafion/LOD/ZnO/Au electrode in the PBS with 0.3 mM L-lactic acid. This peak can be attributed to H_2O_2 generated during L-lactic acid oxidation catalyzed by LOD.[8,26,27] Electrons generated from redox of H_2O_2 through the electrode have enhanced the current response.

Fig. 2c illustrates the CV curves of the Nafion/LOD/ZnO/Au electrode in the PBS with 0.3 mM L-lactic acid at various scan rates of 20, 40, 60, 80, 100 and 120 mV s^{-1}, respectively. The peak currents in the CV curves increase as the scan rate rises, with the arrowhead indicating the increasing direction of the peak current. The inset of Fig. 2c demonstrates that the peak currents increase linearly ($R^2 = 0.9973$) with the square roots of the scan rates (from 20 to 120 mV s^{-1}), which is a typical diffusion-controlled electrochemical behavior.[28]

To study the effect of the ZnO nanotetrapods on the detection performance of the L-lactic acid biosensor, the enzyme electrodes containing ZnO nanotetrapods were tested by amperometric measurements. The corresponding response currents of the Nafion/LOD/ZnO/Au electrode (red curve) and the Nafion/LOD/Au electrode (blue curve) in the L-lactic acid solution are shown in Fig. 3a. In this experiment, L-lactic acid was added once per 100 seconds while being stirred (the concentrations of L-lactic acid added were 0.6 μM and 1.2 μM, 6 μM, 12 μM, 60 μM and 120 μM in A, B, C, D and E regions, respectively) till the response current became stable. The response current rises because of the increase of L-lactic acid concentration. It reaches 90% of the maximum steady-state current within 10 seconds on average. It can be seen from the curve that the electrode with ZnO nanotetrapods shows a faster and more sensitive response than the electrode does without ZnO nanotetrapods as the concentrations of L-lactic acid increase, demonstrating that ZnO nanotetrapods can significantly enhance the current response of the electrodes. It is mainly due to the larger surface area of ZnO nanotetrapods, which results in more adsorption of LOD on the surface of nanotetrapods. It is also attributed to the network of the gathered ZnO tetrapods, which maintains the activity of LOD and provides multiterminal charge transfer channels between enzyme and electrode surfaces. In addition, due to the existence of ZnO nanotetrapods, the background current enhances compared with that of the electrode without ZnO. Consequently, the response current rises slightly when the increase of the L-lactic acid concentration is at the micromole scale. The inset of Fig. 3a (top left) shows that when the concentration reaches 1.2 μM, the response current of the ZnO nanotetrapod bioelectrode displays a step-like profile and turns into 5.7 nA. The current in this case is 7 times as much as it is when 0.6 μM L-lactic acid is added. The current step, when L-lactic acid concentration reaches 1.2 μM, is considered as the first response, which means a detection limit of 1.2 μM of the ZnO nanotetrapod biosensor at a signal-to-noise ratio greater than 3 ($S/N > 3$).

Fig. 3b demonstrates the corresponding calibration curve (solid square) of the L-lactic acid biosensor. As the L-lactic acid concentration increases, the response current is amplified evidently in the linear range from 3.6 μM to 0.6 mM (with $R^2 = 0.9952$) and tends to gradually become stable when the concentration is greater than 1.2 mM. Calculated by means of the slope of the fitted line (shown in the inset of Fig. 3b), the sensitivity of the ZnO nanotetrapod biosensor is 28.0 $\mu A\ cm^{-2}\ mM^{-1}$ ($n = 3$, RSD = 4.9%). The apparent Michaelis–Menten constant ($K_{app,M}$, generally used to estimate the enzymatic bioactivity for a substrate) is calculated from the Lineweaver–Burk equation written as

$$1/i = (K_{app,M}/i_{max})(1/C) + 1/i_{max}$$

where i is the current, i_{max} is the maximum current, and C is the L-lactic acid concentration. The slope of the fitted line in Fig. 3c is 1.024 and $K_{app,M}$ calculated is 0.58 mM, showing an extremely high affinity of the LOD to L-lactic acid in the biosensor.

The stability of the biosensor was acquired by analyzing its CV curves in the presence of 0.3 mM L-lactic acid. After the Nafion/LOD/ZnO/Au electrode (stored at 4 °C) was used 34 times, no obvious decrease of the current was observed based on CV curves.

Furthermore, the sensitivity of the ZnO nanotetrapod bioelectrode is far higher than that of many other L-lactic acid

biosensors reported previously[4,5,10–12,29,30] (enumerated in Table. 1). The low detection limit and relatively lower level linear range make the biosensor particularly suitable for microanalysis. Therefore, this biosensor could analyze suitably diluted blood samples to reflect the health condition of humans. It is worth mentioning that the biosensor in this study is easy to construct and affordable.

3. Conclusions

A new LOD biosensor has been designed based on ZnO nanotetrapods for L-lactic acid detection. The ZnO nanotetrapods are the immobilization substance of LOD on the Au electrode surface. The simple and low-cost biosensor presents a linear response from 3.6 μM to 0.6 mM, a high sensitivity of 28.0 μA cm^{-2} mM^{-1}, a detection limit of 1.2 μM, and a low $K_{app,M}$ of 0.58 mM. The accuracy of the biosensor is achieved by making use of the good biocompatibility of ZnO nanotetrapods, which maintains the activity of enzymes, and the unique multi-terminal electron transmittal feature.

4. Experimental

4.1. Chemicals

L-(+)-Lactate acid (90% solution in water) was purchased from Acros Organics. Nafion solution (5 wt%) and LOD (EC 1.1.3.2, from *Pediococcus* species, lyophilized powders containing 40 units per mg solid) were obtained from Sigma. The reagents were all of analytical grade and used without further purification. 0.1 M PBS was prepared by dissolving NaH_2PO_4 and Na_2HPO_4 into deionized water. LOD solution was prepared by dissolving the LOD lyophilized powder (50 U) into 250 μL of 0.1 M PBS at a pH of 7.4.

4.2. Instrumentation

The morphology and structure of the prepared ZnO nanotetrapods were characterized using scanning electron microscopy (SEM, JEOL-6490), X-ray powder diffraction (XRD, Rigaku DMAXRB) and Raman spectroscopy (JY-HR800). The electrochemical experiment was implemented at room temperature by using an electrochemical workstation (Solartron SI 1287) with a conventional three-electrode system, containing an active electrode we fabricated, an auxiliary electrode of platinum, and an Ag/AgCl reference electrode.

4.3. Preparation of ZnO nanotetrapods

ZnO nanotetrapods were prepared using a vapor phase transport method, which was easy to apply.[22,31] A furnace with a horizontal, long quartz tube inside was utilized. First, ZnO powder with high purity (99.99%) was placed into a small quartz boat, and a slice of silicon wafer as a growing substrate was tied on the quartz boat facing the ZnO powder. Second, the quartz boat was placed in the middle of the quartz tube, and heated at 660 °C for 15 min. Meanwhile, the reaction was proceeding as argon and oxygen went through the quartz tube at a flow rate of 300 sccm (standard cubic centimetre per minute) and 15 sccm, respectively. After the reaction, the quartz boat was taken out and cooled down to room temperature. A kind of synthesized product with a white color was found on the surface of the Si substrate.

4.4. Preparation of Nafion/LOD/ZnO/Au electrodes

A standard gold electrode with a diameter of 2 mm was polished with aluminium slurries, sonicated in deionized water, and then dried under high purity nitrogen gas. To build the L-lactic acid biosensor, 0.5 μL of Nafion solution was firstly dropped on the gold electrode to modify its surface. Then, the prepared ZnO nanotetrapods were dispersed in alcohol, and the suspension was dropped on the surface of the electrode. The suspension was dried in air till ZnO nanotetrapods formed a thin layer. The ZnO layer was wetted by 2 μL of PBS (pH 7.4) and then dried in air. Then 10 μL of LOD solution (2 U) was dropped on the surface of the ZnO/Au electrode and evaporated. Subsequently, 5 μL of Nafion was dropped on the LOD/ZnO/Au electrode and dried in the dark at room temperature for 15 min to form a protective film. The prepared Nafion/LOD/ZnO/Au electrode was stored in a refrigerator at 4 °C.

Acknowledgements

Financial support is acknowledged from the Major Project of International Cooperation and Exchanges (grant no. 2012DFA50990), the National Natural Science Foundation of China (grant nos 51172022, 50972011), the National Natural Science Associate Foundation (grant no. 10876001), the Research Fund of Co-construction Program from Beijing Municipal Commission of Education, the Fundamental Research Funds for the Central Universities, the Beijing Novel Program (2008B19), and the Program for New Century Excellent Talents (NCET-09-0219).

References

1 K. Kriz, L. Kraft, M. Krook, D. Kriz and J. Agric, *J. Agric. Food Chem.*, 2002, **50**, 3419–3424.
2 N. Nikolaus and B. Strehlitz, *Microchim. Acta*, 2008, **160**, 15–55.
3 F. Q. Wu, Y. M. Huang and C. Z. Huang, *Biosens. Bioelectron.*, 2005, **21**, 518–522.
4 M. Mascini, D. Moscone and G. Palleschi, *Anal. Chim. Acta*, 1984, **157**, 45–51.
5 D. Pfeiffer, B. Mollor, N. Klimon and J. Szoponik, *Biosens. Bioelectron.*, 1997, **12**, 539–550.
6 A. Chaubey, K. K. Pande, M. K. Pandey and V. S. Singh, *Appl. Biochem. Biotechnol.*, 2001, **96**, 239–248.
7 S. Suman, R. Singhal, A. L. Sharma, B. D. Malthotra and C. S. Pundir, *Sens. Actuators, B*, 2005, **107**, 768–772.
8 X. Wei, M. Zhang and W. Gorski, *Anal. Chem.*, 2003, **75**, 2060–2064.
9 M. R. Romero, F. Ahumada, F. Garay and A. M. Baruzzi, *Anal. Chem.*, 2010, **82**, 5568–5572.
10 X. Q. Cui, C. M. Li, J. F. Zang, Q. Zhou, Y. Gan, H. F. Bao, J. Guo, V. S. Lee and S. M. Moochhala, *J. Phys. Chem. C*, 2007, **111**, 2025–2031.
11 M. Yang, J. Wang, H. Li, J. G. Zheng and N. N. Wu, *Nanotechnology*, 2008, **19**, 75502–75507.
12 J. Huang, J. Li, Y. Yang, X. Wang, B. Wu, J. Anzai, T. Osa and Q. Chen, *Mater. Sci. Eng., C*, 2008, **28**, 1070–1075.
13 A. Dorfman, N. Kumar and J. Hahm, *Adv. Mater.*, 2006, **18**, 2685–2690.
14 J. Zhao, D. Wu and J. Zhi, *Bioelectrochemistry*, 2009, **75**, 44–49.
15 B. X. Gu, C. X. Xu, G. P. Zhu, S. Q. Liu, L. Y. Chen and X. S. Li, *J. Phys. Chem. B*, 2009, **113**, 377–381.
16 X. L. Ren, D. Chen, X. W. Meng, F. Q. Tang, X. Q. Hou, D. Han and L. Zhang, *J. Colloid Interface Sci.*, 2009, **334**, 183–187.

17 D. Pradhan, F. Niroui and K. T. Leung, *ACS Appl. Mater. Interfaces*, 2010, **2**, 2409–2412.
18 K. Yang, G. W. She, H. Wang, X. M. Ou, X. H. Zhang, C. S. Lee and S. T. Lee, *J. Phys. Chem. C*, 2009, **113**, 20169–20172.
19 M. Ahmad, C. F. Pan, Z. X. Luo and J. Zhu, *J. Phys. Chem. C*, 2010, **114**, 9308–9313.
20 Y. Lei, X. Q. Yan, J. Zhao, X. Liu, Y. Song, N. Luo and Y. Zhang, *Colloids Surf., B*, 2011, **82**, 168–172.
21 Y. Lei, X. Q. Yan, N. Luo, Y. Song and Y. Zhang, *Colloids Surf., A*, 2010, **361**, 169–173.
22 Y. Lei, X. Liu, X. Q. Yan, Y. Song, Z. Kang, N. Luo and Y. Zhang, *J. Nanosci. Nanotechnol.*, 2012, **12**, 513–518.
23 J. M. Calleja and M. Cardona, *Phys. Rev. B: Solid State*, 1977, **16**, 3753–3761.
24 Y. Dai, Y. Zhang, Q. K. Li and C. W. Nan, *Chem. Phys. Lett.*, 2002, **358**, 83–86.
25 M. I. Guzman and S. T. Martin, *Astrobiology*, 2009, **9**, 833–842.
26 Y. Yang, H. Yang, M. Yang, Y. Liu, G. Shen and R. Q. Yu, *Anal. Chim. Acta*, 2004, **525**, 213–220.
27 L. Zhang and S. Dong, *J. Electroanal. Chem.*, 2004, **568**, 189–194.
28 J. X. Wang, X. W. Sun, A. Wei, Y. Lei, X. P. Cai, C. M. Li and Z. L. Dong, *Appl. Phys. Lett.*, 2006, **88**, 233106.
29 N. F. Shram, L. I. Netchiporouk, C. Martelet, J. R. Nicole, C. Bonnet and R. Cespuglio, *Anal. Chem.*, 1998, **70**, 2618–2622.
30 J. Yan, V. A. Pedrosa, A. L. Simonian and A. Revzin, *ACS Appl. Mater. Interfaces*, 2010, **2**, 748–755.
31 H. F. Li, Y. H. Huang, Y. Zhang, J. J. Qi, X. Q. Yan, Q. Zhang and J. Wang, *Cryst. Growth Des.*, 2009, **9**, 1863–1868.